

---

## Orientation and spatial frequency selectivity following adaptation: A reaction time study

---

Sotiris Plainis<sup>1,2</sup>, Neil R A Parry<sup>3,4</sup>, Panagiotis Sapountzis<sup>5</sup>, Ian J Murray<sup>2</sup>

<sup>1</sup>Institute of Vision and Optics (IVO), University of Crete, 71003 Heraklion, Crete, Greece;

<sup>2</sup>Faculty of Life Sciences, University of Manchester, Manchester, UK; <sup>3</sup>Centre for Hearing and Vision Research, Institute of Human Development, University of Manchester, Manchester, UK; <sup>4</sup>Vision Science Centre, Manchester Royal Eye Hospital, Central Manchester University Hospitals NHS Foundation Trust, Manchester Academic Health Science Centre, Manchester, UK;

<sup>5</sup>Institute of Applied and Computational Mathematics, Foundation for Research and Technology, Hellas (FORTH), 71003 Heraklion, Crete, Greece; e-mail: plainis@med.uoc.gr

Received 10 June 2014, in revised form 8 December 2014, published online 5 March 2015

---

**Abstract.** The aim of the study was to determine orientation and spatial frequency sensitivity using reaction times (RTs) in an adaptation paradigm. Simple RTs were measured to the onset of a Gabor patch ( $SD = 1.2$  deg, spatial frequency =  $4$  cycles  $\text{deg}^{-1}$ ). Observers adapted for  $10$  s to a  $4$  cycles  $\text{deg}^{-1}$  grating presented at a series of orientations ( $0, 2, 5, 10, 22.5, 45, 90^\circ$ ) or spatial frequencies ( $\pm 0.5, 1, 2$  octaves). The contrast of the test grating was  $4\times$  each participant's unadapted threshold. The effect of adaptation was evaluated by transforming RTs to effective contrast reduction using RT-based contrast response functions. RTs increased by between  $\sim 100$  ms to  $150$  ms when the test and adapting gratings were of the same orientation or spatial frequency. The effect became less pronounced as the difference in orientation or spatial frequency increased. The average bandwidths for orientation and spatial frequency were  $17.4^\circ$  and  $1.24$  octaves, respectively. The method has some advantages over traditional approaches. It reveals a rapid time course of adaptation recovery with a half-life of about  $13$  s to  $23$  s. RTs form a rapid and easily implemented technique for assessing the underlying physiological mechanisms that control adaptation at suprathreshold levels of contrast.

**Keywords:** adaptation, contrast, reaction time, spatial frequency, orientation

### 1 Introduction

A general characteristic of sensory nervous systems is that they exhibit a decline in response after continuous exposure to the same stimulus. This helps highly dynamic processes to efficiently encode stimuli whose physical parameters vary in time (Kohn, 2007). In the visual system prolonged viewing of a high-contrast pattern induces a substantial rise in detection threshold (Blakemore & Campbell, 1969a). In humans, electrophysiological and psychophysical studies have shown that sensitivity to a test grating is temporarily reduced by masking gratings presented concurrently (Campbell & Kulikowski, 1966; Ross & Speed, 1991; Sekuler, 1965; Stromeyer, Klein, Dawson, & Spillmann, 1982; Tolhurst & Barfield, 1978) or by adapting gratings presented for some period before the appearance of the test stimulus (Blakemore & Campbell, 1969a; Blakemore & Nachmias, 1971; De Valois, 1977; Georgeson & Harris, 1984; Greenlee, Georgeson, Magnussen, & Harris, 1991; Greenlee & Heitger, 1988; Heinrich & Bach, 2002; Ross & Speed, 1991).

The decreased sensitivity following adaptation shows partial interocular transfer (Blakemore & Campbell, 1969b) and is confined to patterns of similar spatial frequency (Blakemore & Campbell, 1969b; Blakemore, Muncey, & Ridley, 1973; Wilson & Humanski, 1993) and orientation of the adapting pattern (Blakemore & Nachmias, 1971; Gilinsky, 1968). As the difference in spatial frequency or orientation between the adapting and the test grating increases, the desensitisation caused by adaptation is reduced. This reduction in sensitivity can be used to derive orientation and spatial frequency tuning functions. The bandwidth of adaptation

---

effects in the orientation domain, usually calculated as full-width half maximum (FWHM), has been reported to range between 8° (Blakemore & Nachmias, 1971; Gilinsky, 1968) and 45° (Greenlee & Magnussen, 1988). However, bandwidths can vary depending on the technique used to measure selectivity (De Valois & De Valois, 1990).

Adaptation-based spatial frequency bandwidths are estimated to be approximately one octave (Blakemore & Campbell, 1969b; Stecher, Sigel, & Lange, 1973). There are suggestions (De Valois, 1977; Tolhurst & Barfield, 1978) that sensitivity to the test grating may also be enhanced when its spatial frequency differs by more than 2 octaves from the adapting grating. This effect is convincingly described by De Valois (1977), who showed an enhancement in contrast sensitivity for gratings whose spatial frequency differed from the adapting stimulus by 2–3 octaves. This suggests some form of mutual inhibitory interactions among spatial frequency detectors.

Psychophysical approaches used to evaluate adaptation effects usually rely on being able to obtain a threshold setting rapidly because when the adapting stimulus is withdrawn, thresholds fall quickly. As is well known, accurate determination of threshold takes a finite time (Campbell & Kulikowski, 1966), and there is a trade-off between accuracy and time taken. If the threshold measure takes more than one minute or so, sensitivity is likely to have improved markedly during the measurement time. Adaptation can operate over many different time scales, depending on the site of the adaptation (Baccus & Meister, 2002; Duong & Freeman, 2007; Webster, 2011; Yeh, Lee, & Kremers, 1996), and the time taken to determine threshold may therefore be a confounding factor in measuring adaptation effects. Thus, some methods have been advanced to allow instantaneous measurements of threshold, like the method of a thousand staircases (Anderson & McKendrick, 2007; Mollon & Polden, 1980; Pianta & Kalloniatis, 2000). While these methods have relatively high temporal resolution (typically 2 s), they require many repetitions of the entire paradigm in order to establish a series of thresholds.

Parry, Murray, and McKeefry (2008) introduced a technique which has sufficiently high temporal resolution to address this issue. They used simple reaction times (RTs) to monitor the effects of adaptation, which allowed the time course of the effects to be mapped over a wide range of contrasts. One particular advantage of measuring sensitivity using the RT is that it is suprathreshold, and thus more closely related to real-world conditions. It has been known for many years (eg Harwerth & Levi, 1978; Palmer, Huk, & Shadlen, 2005; Taylor, Carpenter, & Anderson, 2006) that RTs exhibit a robust relationship with stimulus contrast. Furthermore, it has been shown that RTs can be used to selectively monitor either magnocellular (M) or parvocellular (P) detecting mechanisms (Murray & Plainis, 2003; Plainis & Murray, 2000, 2005). Over a wide range of contrast, spatial frequency, and luminance, RT-based measures of contrast gain closely matched those of the M and P cells in the macaque monkey (Ohzawa, Sclar, & Freeman, 1982; Sclar, Lennie, & DePriest, 1989). Plainis and Murray (2000) showed that a linear relationship exists between RTs and inverse contrast, allowing them to be used as a suprathreshold surrogate for contrast sensitivity. This assumption formed the basis of the RT adaptation technique devised by Parry et al. (2008). If sensitivity to a particular stimulus is reduced by adaptation, there is a concomitant increase in RT. Parry et al. introduced the concept of 'effective contrast reduction', relating the increase in RT directly to contrast reduction using each individual's RT versus inverse-contrast function. Because each individual RT is related (with finite confidence limits) to sensitivity, even a single run of RTs recorded following adaptation could characterise the time course of recovery. Parry et al. (2008) illustrated the technique by showing contrast-dependent adaptation of a same-axis colour mechanism, which was absent when adaptation was along the orthogonal chromatic axis. The time course of recovery from adaptation seemed to show both slow and fast phases, in line with studies on macaque retinal ganglion cells (Yeh et al., 1996)

and more recent behavioural studies (Bao & Engel, 2012). Of course, all adaptation paradigms implicitly assume that the effects reflect in some way the activity of groups of neurons. Hegde (2009) used a simple neuronal ensemble model of spatial frequency processing to test whether adaptation bandwidth obtained psychophysically was related to bandwidth at the neural level. He found that the adaptation level was independent of spatial frequency tuning and that different spatial frequency tuning produced the same adaptation bandwidths. It seems that system-level bandwidths may not be as closely related to neuronal bandwidth as at first thought.

Notwithstanding these observations, all the above suggest that RTs may be a valuable probe of the mechanisms underlying sensory adaptation in the human visual system. The objective of the present work was to use the Parry et al. (2008) technique to provide data on contrast adaptation, by measuring visual RTs before and after short bursts of adaptation to a suprathreshold grating. Hence, three aspects of the effects of an adapting grating stimulus are investigated: (a) orientation selectivity, (b) spatial frequency selectivity, and (c) the dynamics of adaptation and adaptation recovery.

## 2 Methods

### 2.1 Subjects

Data were obtained from the dominant eye of five male participants: SP, NK, VZ, IJM, and GB, aged 36, 29, 24, 61, and 23 years, respectively. All participants were experienced observers: SP and IJM are authors. All participants had a visual acuity equal to or better than 6/5. Where required, spectacle correction was used. SP participated in both experiments, whilst NK and VZ participated in experiment 1 and IJM and GB in experiment 2. Written informed consent was obtained from the participants. The research conformed to the tenets of the Declaration of Helsinki and followed a protocol approved by the University of Crete Institutional Research Ethics Board.

### 2.2 Stimuli

Both test and adapting stimuli consisted of achromatic symmetric Gabor patches (Gaussian-windowed sinusoidal gratings) with a standard deviation of 1.2 deg at 2.5 m distance. They were displayed on a Sony 21-inch GDM F-520 CRT (frame rate = 120 Hz) by means of a VSG 2/5 stimulus generator card (Cambridge Research Systems Ltd, Rochester, UK). Mean screen luminance was 30 cd m<sup>-2</sup>. Contrast was defined in terms of Michelson—that is:

$$C = \frac{L_{\max} - L_{\min}}{L_{\max} + L_{\min}}, \quad (1)$$

where  $L_{\max}$  and  $L_{\min}$  are the respective luminance maxima and minima of the stimulus, and is presented here in dB, where:

$$C(\text{dB}) = -20 \log_{10}(C). \quad (2)$$

The gamma functions of the red, green, and blue guns of the monitor were calibrated with a colorCAL (Cambridge Research Systems Ltd, Rochester, UK) and checked with a PR-650 spectroradiometer (PhotoResearch, Chatsworth, CA).

Two experiments were performed. In all conditions the test grating was modulated with a square wave temporal window of 380 ms duration and had a spatial frequency of 4 cycles deg<sup>-1</sup> and vertical orientation (90°). The contrast of the test grating was a fixed amount above each participant's threshold (see below). The background was of the same mean luminance and hue as a zero contrast grating. Mean luminance of the Gabor at  $C = 1.0$  was within 0.001% of the background luminance.

In the first experiment the static adapting grating was presented for 10 s at one of a series of orientations which differed from the test grating by  $-90$ ,  $-45$ ,  $-22.5$ ,  $-10$ ,  $-5$ ,  $-2$ ,  $0$ ,  $2$ ,  $5$ ,  $10$ ,  $22.5$ ,  $45$ , and  $90^\circ$ . Spatial frequency was always  $4 \text{ cycles deg}^{-1}$ . The contrast of the adapting grating was  $14 \text{ dB}$  ( $0.2$ ) to minimise the occurrence of luminance afterimages. This was chosen because higher contrasts induced a strong afterimage of the pattern affecting the visibility of the test grating (Plainis, Parry, Sapountzis, Murray, & Pallikaris, 2006). In control experiments we found that, regardless of whether the adaptor was static or reversing, the adaptation was always the same probably due to the spatial frequency ( $4 \text{ cycles deg}^{-1}$ ) chosen. Adapting with a static grating had a marked effect on adaptation only at low spatial frequencies ( $\leq 2 \text{ cycles deg}^{-1}$ ).

In the second experiment a contrast-reversed adapting pattern, temporally modulated at  $1 \text{ Hz}$ , was chosen to eliminate luminance afterimages. Its orientation was constant ( $90^\circ$ ) and its spatial frequency was varied ( $0$ ,  $0.5$ ,  $1$ ,  $1.5$ , and  $2$  octaves above and below  $4 \text{ cycles deg}^{-1}$ ; see table 1). The contrast of each adapting spatial frequency was determined according to the RT versus contrast function, described below. RTs are known to vary systematically with spatial frequency and contrast (Plainis & Murray, 2000). Hence, for each observer, a contrast for the adapting grating, which corresponded to equal (same) suprathreshold RT for each spatial frequency, was selected. For example, for NK an RT to  $14 \text{ dB}$  at  $4 \text{ cycles deg}^{-1}$  is equal to an RT of  $3 \text{ dB}$  at  $1 \text{ cycle deg}^{-1}$ , of  $12 \text{ dB}$  at  $8 \text{ cycles deg}^{-1}$ , and of  $2 \text{ dB}$  at  $16 \text{ cycles deg}^{-1}$ . The contrasts of the adapting gratings for the range of spatial frequencies used are given for each subject in table 1.

**Table 1.** The contrast level (in dB) of the adapting grating corresponding to equal (same) suprathreshold reaction time for each spatial frequency.

Spatial frequency/ cycle $\text{deg}^{-1}$	Participant		
	SP	GB	NK
1.0	5	6	3
1.4	11	8	7
2.0	12	11	12
2.8	13	14	13
3.4	13	15	13
4.0	14	14	14
4.8	13	14	13
5.6	13	11	12
8.0	10	10	11
11.3	7	6	10
16.0	0	0	2

## 2.3 Procedure

**2.3.1 Suprathreshold test contrast determination.** The contrast threshold for the test grating was determined for each participant using a binary-search staircase with a resolution of  $1 \text{ dB}$ . Initially, the stimulus (modulated at  $1 \text{ Hz}$ ) was presented with a contrast of  $32 \text{ dB}$ . If the stimulus was detected, contrast was decreased by  $16 \text{ dB}$ ; otherwise, it was increased by  $16 \text{ dB}$ . Once detection had occurred, successive increments were halved until the increment was less than  $1 \text{ dB}$ , and the resultant contrast was taken as the threshold. The average of four runs,  $\theta$ , was taken as threshold. The contrast of the test grating used for each participant in the adaptation experiments was always  $4\theta$  (ie  $12 \text{ dB}$  higher than threshold).

**2.3.2 RT versus contrast functions.** Prior to the main experiment, a function of RT versus contrast was derived for each subject in a single run with 64 stimuli being presented in equal intervals between full contrast and threshold on a  $1/\text{contrast}$  scale. The method is described in a previous study (Parry, Plainis, Murray, & McKeefry, 2004); characteristic data for subject SP are presented in figure 1. Each stimulus was presented after an equal-likelihood random interval of between 1000 ms and 3000 ms. If no response was made, the inter-stimulus interval was 5000 ms. The technique is quick, each RT versus contrast function being obtained in around 3 min. The slope of the resulting RT versus  $1/\text{contrast}$  function has been used as a measure of the RT-based sensitivity (Parry et al., 2004; Plainis & Murray, 2000). In this study it was used to derive the reduction in effective contrast from the increase in RTs following adaptation. See Parry et al. (2008) for a full description of this procedure. In figure 1 a particular increase in RT (from 307 ms to 368 ms) is shown to correspond to a change in reciprocal contrast from 53 to 95, which represents an effective contrast reduction of approximately 5.0 dB (from 34.5 dB to 39.5 dB).

The RT data were transformed to equivalent contrast reduction using the following expression:

$$\text{Reduction (dB)} = \frac{RT_a - RT_0}{k}, \quad (3)$$

where  $RT_a$  = RT during adaptation,  $RT_0$  = RT prior to adaptation, and  $k$  = slope of RT versus  $1/\text{contrast}$  function.

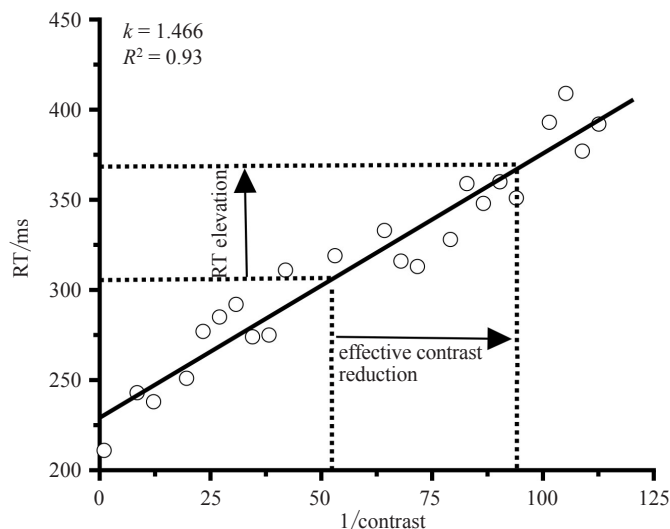


**Figure 1.** Plot of reaction time (RT) versus the reciprocal of contrast for a grating of 4 cycles  $\text{deg}^{-1}$  spatial frequency and  $90^\circ$  orientation (subject SP). For this specific condition extrapolating the adapted RT back to the RT versus  $1/\text{contrast}$  plot gives a measure of effective contrast reduction. More specifically, an RT elevation of 61 ms following adaptation (from 307 ms to 368 ms) corresponds to a change in reciprocal contrast from 53 to 95, which equates an effective contrast reduction of 5.0 dB.

**2.3.3 Adaptation.** In the main experiment, illustrated schematically in figure 2, simple RTs were measured to the onset of the test grating. Subjects pressed a button (CB6 box, Cambridge Research Systems Ltd, Rochester, UK) as soon as they saw the stimulus. Timing was obtained from the VSG card with resolution higher than 1 ms. A typical experiment consisted of a single run with three phases. In the baseline phase 32 RTs were recorded without adaptation. Prior to the presentation of each individual stimulus, there was a foreperiod with an equal-likelihood random interval between 1500 ms and 2500 ms. In the adaptation phase 32 RTs were again recorded but the random foreperiod was preceded by a 10 s presentation

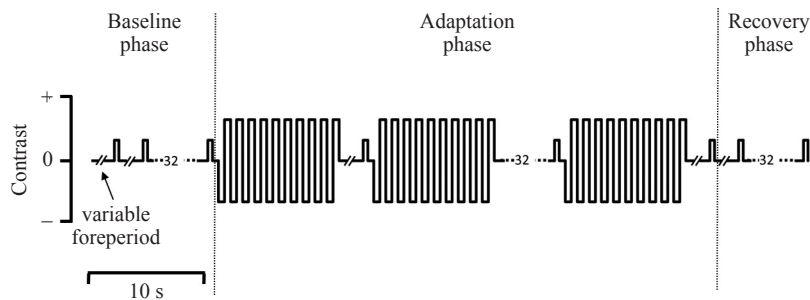


**Figure 2.** Reaction time (RT) experimental paradigm for spatial frequency adaptation. During the baseline phase RT was measured to the onset of a 380 ms (test) grating, presented 32 times. During the adaptation phase 32 RTs were again recorded, each of which was preceded by a 10 s presentation of the adapting grating. The recovery phase consisted of 32 presentations of the test grating. In all phases, prior to the presentation of each individual stimulus, there was a variable foreperiod with an equal-likelihood random interval between 1500 ms and 2500 ms. The orientation paradigm was the same except that the adapting grating was static.

of the adapting grating. Three seconds after the subject's responses the adapting stimulus reappeared. If no response was made, the interstimulus interval was 3000 ms. The third phase ('recovery') consisted of 32 responses without adaptation. Only one experiment (varying orientation in 9 runs or spatial frequency in 13 runs) was conducted in each session. With 5 min breaks between each run, the total length of the experiment was about 2 to 3 h.

Averages of 32 responses for the baseline and adaptation conditions were compared. Early (<250 ms) or late responses (>700 ms) were excluded from further analysis. Outliers from the main distribution were removed by excluding data greater than 2 standard deviations. No more than 6 data points were removed from any single experiment.

### 3 Results

Figure 3 illustrates raw RTs derived from four superimposed sessions (for a single subject), during and following a 10 s exposure to a 14 dB adapting grating of the same orientation ( $90^\circ$ ) and spatial frequency ( $4 \text{ cycles deg}^{-1}$ ) as the test grating. Contrast of the test grating was 12 dB higher than the threshold. It is evident that, for these conditions, adaptation results

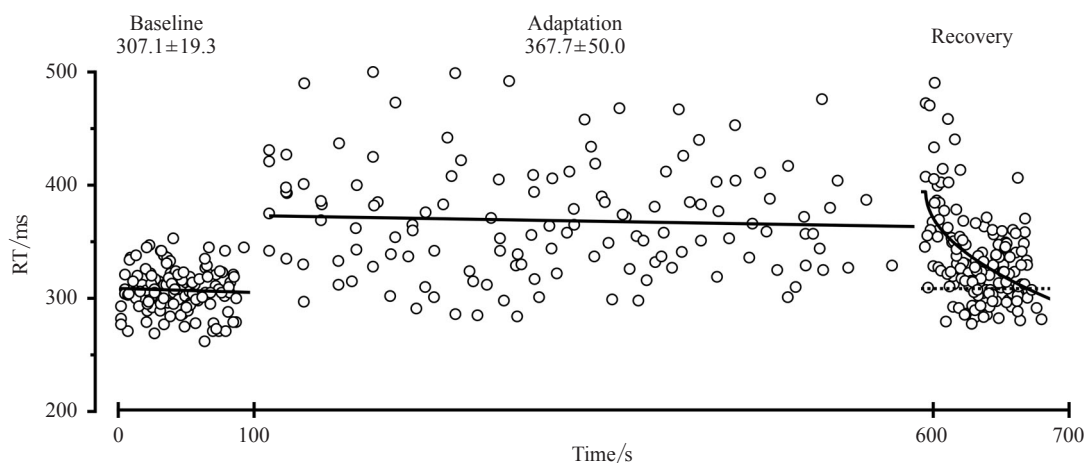


**Figure 3.** Reaction times (RTs) before, during, and after adapting to a 20% contrast grating. Four superimposed recordings from one subject are presented. The orientation of the test and the adapting gratings was  $90^\circ$ , and their spatial frequency was  $4 \text{ cycles deg}^{-1}$ . The solid lines are best-fitted linear regression fits in the baseline and adaptation phase and a power function in the recovery phase. Mean RT ( $\pm$  standard errors) is shown above the first two phases. These values are used in figure 1.

in an average elevation in RT from 307.1 ms at baseline to 367.7 ms. On the basis of this observer's RT versus  $1/C$  function, this increase in RT (60.6 ms) corresponds to an effective contrast reduction of 5.0 dB. This is the example given in figure 1. Standard deviation also increased during the adapting phase, from 19.3 ms to 50.0 ms. The RT following removal of the adapting grating returned gradually to preadapted values. Note that the slopes of the linear regression fits to the RT versus time data during the 100 s of baseline and the 500 s of adaptation phases are not significantly different from zero (Pearson's correlation coefficient,  $r$ , equals  $-0.04$ ,  $p = 0.65$ , and  $-0.05$ ,  $p = 0.58$ , respectively). This shows that, during the adaptation phase of the experiment, there was no slow build-up of adaptation from the 'top-up' procedure; this seemed complete from the outset, as was also observed in studies of chromatic adaptation (Parry et al., 2008).

#### 4 Experiment 1: adaptation and orientation tuning

In figure 4 we present in more detail the effect of varying the orientation of the adapting grating. The upper panel shows raw data, with empty symbols depicting the nonadapted RTs and filled symbols the adapted RTs. When the orientation difference between the adapting and the test grating is zero, the highest increase in RT is produced (62 ms for subject SP, 42 ms for subject VZ, and 70 ms for subject NK) (see lower panel in figure 4). As expected, the orientation of the adapting grating relative to the test has an effect on the amount of adaptation. When the adaptor was oriented orthogonally to the test the effect of adaptation was minimal. The orientation tuning curves were modelled using best-fitted Lorentzian peak functions in conjunction with a first or second-order polynomial background. A background component was introduced to account for the asymmetries on the two sides of the distribution.

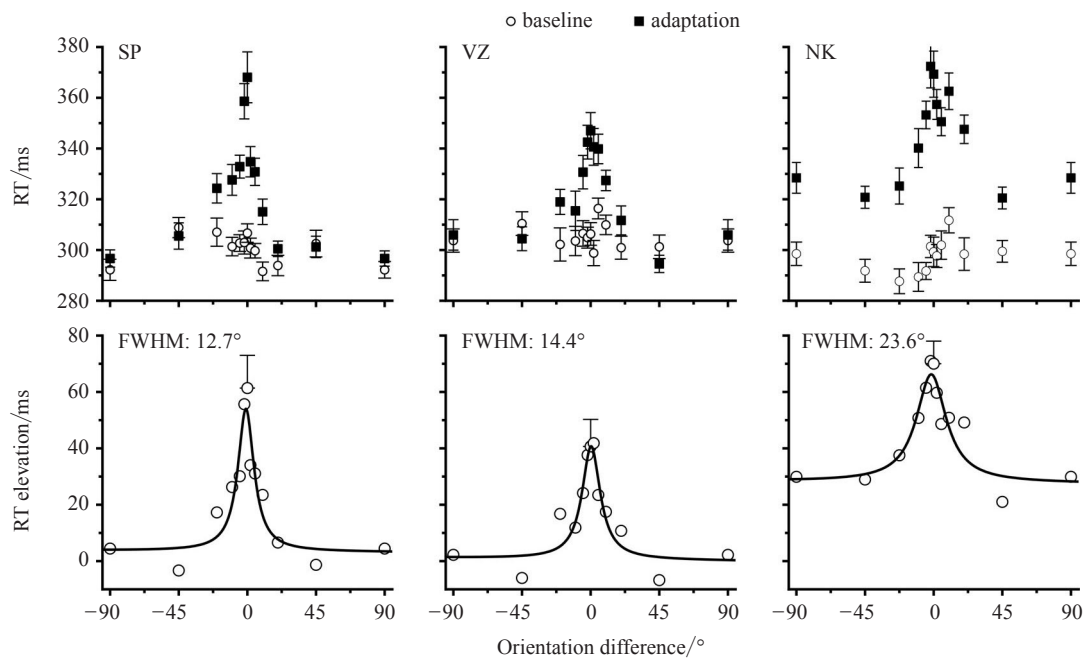


**Figure 4.** Plots of reaction time (RT) (upper) and RT elevation (lower) for the adaptation (open circles) and the baseline (filled squares) conditions, as a function of the difference in orientation between the adapting and the test grating. The spatial frequency of the adapting and the test grating was  $4 \text{ cycles deg}^{-1}$ , while the orientation of the latter was  $90^\circ$ . The solid lines are best-fitted Lorentzian functions. The value in the legend corresponds to the full-width half maximum (FWHM) (in  $^\circ$ ). Each data point (upper graph) represents the mean of at least 26 measurements (32 maximum) and the error bars  $\pm 1$  standard error. The error bar in the lower graphs indicates the standard deviation for 4 trials, repeated only for one condition ( $0^\circ$ ).

The fitted function was always selected to peak at zero ( $x_0 = 0$ ), since this denotes the difference in orientation and spatial frequency between the adapting and the test gratings and corresponds to the theoretically predicted maximum adaptation. The Lorentzian function ( $L$ ) was defined as:

$$L = \frac{A}{1 + \left(\frac{x - x_0}{s}\right)^2} + \sum_{i=0}^2 b_i x^i, \quad (4)$$

where  $s$  is a scale parameter that specifies the half width at half maximum,  $A$  and  $x_0$  are parameters specifying the amplitude and location of the peak respectively, and  $b_i$  are the coefficients of the background polynomial.

The bandwidth of the orientation tuning functions in terms of RT, measured at FWHM, was  $12.7^\circ$  for subject SP,  $14.4^\circ$  for subject VZ, and  $23.6^\circ$  for NK. However, these values reflect differing amounts of effective contrast loss for each individual because their RT versus  $1/C$  functions (see example, in figure 1) have different slopes. It is therefore important to assess the difference between the adapting and nonadapting conditions from an estimate of sensitivity loss as described in section 2 and in figure 1. The slope of RT versus  $1/C$  functions (see figure 1a) allows the RT elevation to be transformed to effective contrast reduction in dB [see equation (3)]. The results of this transformation, fitted with Lorentzian functions [equation (4)], are presented in figure 5. The bandwidth of the orientation tuning functions in terms of contrast, measured at FWHM, was  $21.6^\circ$  for subject SP,  $17.2^\circ$  for subject VZ and  $28.8^\circ$  for subject NK. These values compare favourably with those obtained from threshold experiments and from contrast matching experiments (eg Blakemore et al., 1973). The extent of maximal contrast loss varied between observers, with SP showing a loss of 5.1 dB, VZ showing a loss of 4.3 dB, and NK showing a loss of 5.5 dB.

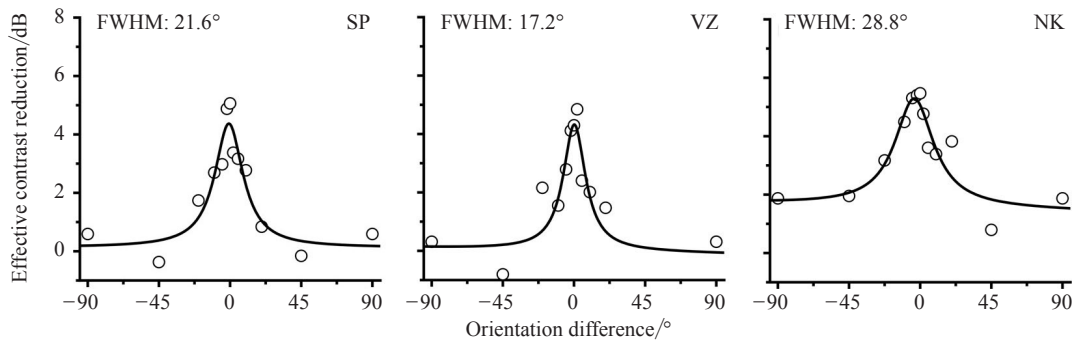


**Figure 5.** Plots of effective contrast reduction (in dB) as a function of the difference in orientation (in  $^\circ$ ) between the adapting and the test grating. The value in the legends corresponds to the FWHM (in  $^\circ$ ) as calculated by the best-fitted Lorentzian functions (solid lines). Effective contrast reduction was estimated from the RT versus  $1/C$  plots (see figure 1).

## 5 Experiment 2: adaptation and spatial frequency tuning

Figure 6 presents tuning functions in the spatial frequency domain. These have been derived in the same way as those in figures 4 and 5. As described above, the contrast of each adapting grating was chosen so as to produce the same RT. Corresponding values for each observer are illustrated in table 1. It is evident again that the elevation in RT is maximal when the test and the adapting grating are of the same spatial frequency, being less pronounced when the adapting grating differed in spatial frequency from the test grating. The perceived contrast loss, interpreted in terms of best-fitted Lorentzian functions, reveals tuning curves having a bandwidth of 1.68 octaves for subject SP, 1.07 octaves for subject IJM, and 1.70 octaves for subject GB.

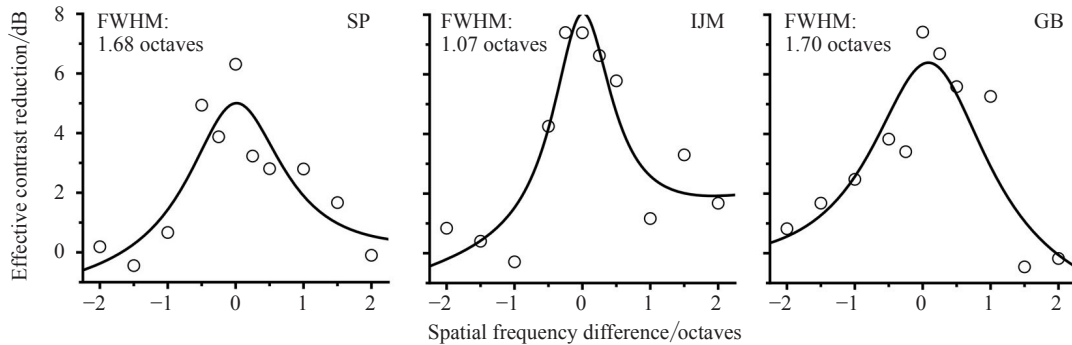


**Figure 6.** Plots of effective contrast reduction (in dB) as a function of spatial frequency (in octaves) for three subjects. The value in the legends corresponds to the full-width half maximum (FWHM) value (in octaves) as calculated by the best-fitted Lorentzian functions (solid lines).

## 6 Comparing adaptation with orientation and spatial frequency

Figure 7 illustrates the effects of the adapting stimuli in terms of effective contrast reduction, comparing the spatial frequency with orientation and averaging across the three subjects. The average bandwidths were  $17.4^\circ$  and 1.24 octaves for orientation and spatial frequency tuning functions, respectively. Note that, for orientation adaptation, the condition of a  $45^\circ$  difference between adaptor and test appears to induce the lowest elevation in the RT, indicating facilitatory interactions.

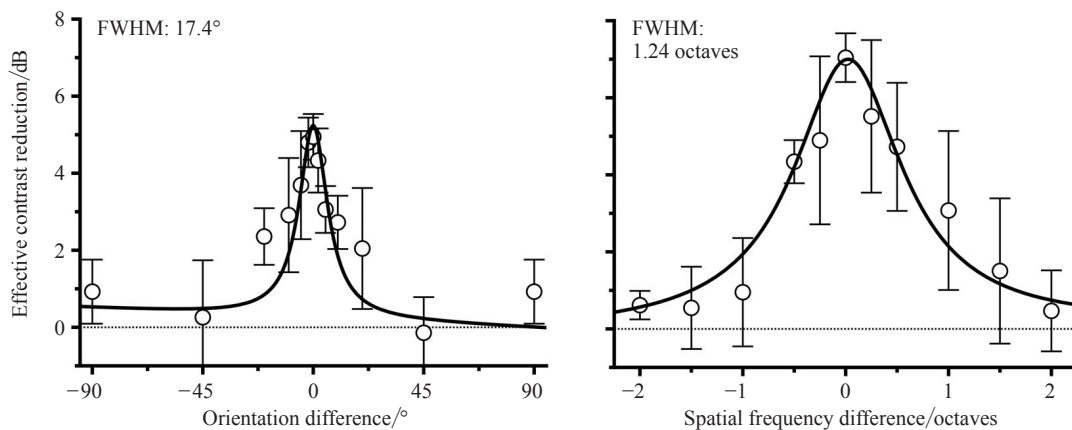


**Figure 7.** Average tuning plots in orientation (left) and spatial frequency (right) across the three observers for the two experimental adaptation conditions. The values in the legends correspond to the full-width half maximum (FWHM) in degrees and octaves, respectively. The error bars indicate  $\pm 1$  standard deviation.

## 7 Time course of the effect of adaptation

One of the advantages of the RT-based method in evaluating adaptation is that the time course of the onset and recovery of the adaptation can be explicitly measured even in a single experiment. In figure 8 we show how the technique can be used to measure the decay of the adaptation effect. The effect of adaptation was greatest immediately after adaptation and decayed rapidly thereafter. Exponential functions have been fitted to the averaged data (bins of 10 s) from experiment 1 to estimate the half-life of the recovery from orientation adaptation, which was found to vary notably between the three subjects from 13.5 s for subject VZ to 18.8 s for NK and 23.0 s for SP. This is in line with prior reports of the decay of contrast adaptation (Bao & Engel, 2012; De Valois, 1977; Greenlee et al., 1991; Greenlee & Heitger, 1988). For example, De Valois (1977) reported substantial interindividual variations and the fact that observers' performance in adaptation tasks changes with practice.

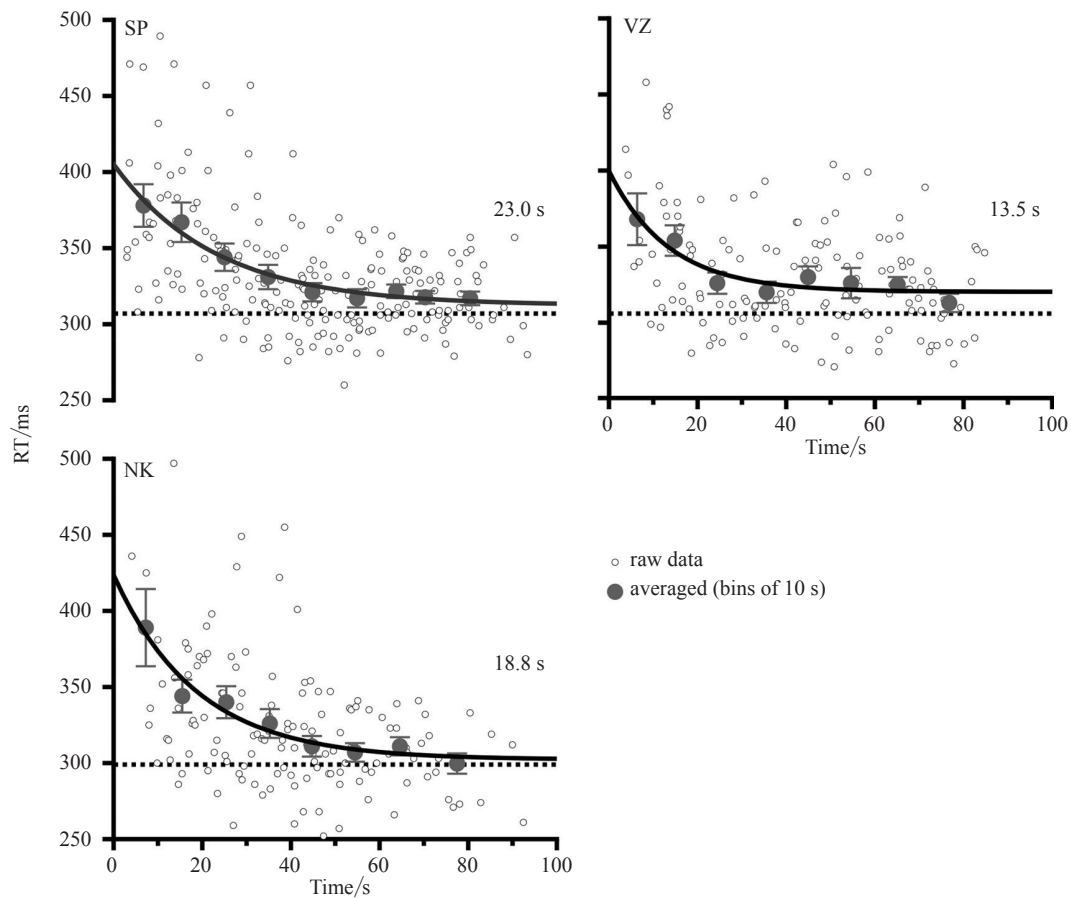


**Figure 8.** Plots of reaction time (RT) as a function of time during the recovery period following orientation adaptation for the three subjects in experiment 1. Each graph includes data from four runs for maximum adaptation—that is, test and adapting gratings of same orientation ( $90^\circ$ ) and spatial frequency ( $4 \text{ cycles deg}^{-1}$ ). Small circles represent raw data whereas filled circles correspond to averaged data into bins of 10 s. The legend indicates the half-life of recovery from the adaptation fitted by exponential functions (solid lines). The error bars indicate  $\pm 1$  standard error. Dotted lines correspond to the unadapted baselines.

## 8 Discussion

Simple RTs were recorded prior to, during, and after a period of pulses of adaptation to a series of sinusoidal gratings of different orientations and spatial frequencies. The effect of the adaptation was calculated by transforming RT data to effective contrast reduction from RT-based contrast response functions obtained for each observer. This allowed the estimation of bandwidths of the underlying physiological mechanisms. Furthermore, the use of RTs to evaluate adaptation allows the study of adaptation at suprathreshold contrast levels. Under normal everyday viewing conditions, all patterns are above threshold, and it is argued that it is more important to understand the properties of the underlying mechanisms under these conditions than at threshold.

It has also been suggested that adaptation effects are increased by sustained attention to the adapting stimulus (Ling & Carrasco, 2006; Morgan, 2011), leading to increased contrast thresholds. Similarly, RT measures, which are prone to expectancy effects, may be influenced. In the current experiment participants were experienced observers. We also chose a random interleaving between the adapting and the test grating conditions, while a low-contrast adaptor was used. These should minimise any effects of cognitive and response biases (Morgan, 2013).

---

### 8.1 *Adaptation effects in orientation*

As expected, stronger adaptation effects were observed when the test and adapting grating had the same orientation. There is a suggestion that some form of facilitation occurs when the test and adapting grating differ by  $45^\circ$ , and this effect seems to be present for all three observers, as illustrated in figure 5. Previous work (De Valois, 1977; Greenlee & Magnussen, 1988) has reported such facilitatory interactions in both orientation and spatial frequency domain adaptation profiles. Greenlee and Magnussen (1988) observed enhancement effects when the orientation and the spatial frequency difference between the adapting and the test grating were approximately  $45^\circ$  or 1.5 octaves, respectively. Our results reflect these observations.

Overall, the results of the RT-based adaptation technique are in agreement with the tuning functions derived from threshold and masking experiments. Bandwidths of around  $17^\circ$  to  $29^\circ$  are obtained, as illustrated in figures 5 and 7. Blakemore and Nachmias (1971) and Blakemore et al. (1973) obtained somewhat lower values; the latter used  $8.4 \text{ cycles deg}^{-1}$  and obtained a bandwidth of  $8^\circ$ .

### 8.2 *Adaptation effects in spatial frequency*

When spatial frequency tuning functions are generated from threshold-based data, the bandwidth is around 0.8 octave, according to Blakemore and Campbell (1969b). De Valois (1977) found narrower and more symmetrical spatial selectivity, with a mean bandwidth of around 0.68 octave. The main subject in that study was highly trained, having repeated the experiments many times over an 1.5-year period. It was conceded that, with practice, the performance of observers changed so that tuning curves became narrower. De Valois used a larger field and higher luminance than Blakemore and Campbell (1969a), but these factors were not thought to explain the differences between the two datasets. Stromeyer and Julesz (1972) obtained slightly wider tuning functions using filtered one-dimensional noise to mask test gratings. Since bandwidths may vary depending on the technique used to measure selectivity and the metrics applied to evaluate the adaptation effect, it is not surprising that spatial frequency bandwidth values vary significantly across different studies.

In our study the RT technique produced tuning functions with bandwidths very similar to this, with a mean bandwidth of 1.24 octaves when data are averaged over the three subjects. Of course, these bandwidths may be regarded as a little too wide to support classical spatial frequency tuning; but, as pointed out by Tolhurst (1972), this may be because spatial frequency channels inhibit each other, the aftereffects of adaptation being the tuning characteristics of this inhibition rather than the excitatory tuning characteristics themselves. As discussed in De Valois and De Valois (1990), the visual system does not perform the global analysis required for idealised frequency analysis. There is, however, anatomical and physiological evidence that each cortical module is composed of cells tuned to many spatial frequencies. It would appear that the system performs a form of analysis that can be regarded as the optimum between the two extremes of space and spatial frequency, and there is a sound theoretical basis for this (Daugman, 1985). The narrowness of the filters measured with any particular technique is therefore of some practical and theoretical importance. The issues related to channel bandwidth, independence of channels and their possible role at suprathreshold contrast, are reviewed in Klein (1991).

### 8.3 *Recovery from adaptation*

In the current study we investigated adaptation effects with high temporal resolution. A brief 5 min adaptation period in a top-up manner produced a moderate increase in RT (reduction in effective contrast) that decayed quickly—that is, the half-life of the decay of adaptation was about 13–23 s. This is in agreement with threshold studies (Bao & Engel, 2012; Bao, Mesik, & Engel, 2013; Greenlee et al., 1991), which employed similar adaptation durations.

---

Effects of contrast adaptation get stronger and longer-lasting as the adapting duration lengthens (Bao & Engel, 2012; Greenlee et al., 1991; Wark, Fairhall, & Rieke, 2009). Bao and Engel (2012) and Bao et al. (2013) showed that contrast adaptation is possibly controlled by multiple distinct mechanisms acting over a large range of time scales. Similar observations were made in Parry et al.'s (2008) RT adaptation study.

#### 8.4 *Site of adaptation*

It is generally thought that selective adaptation arises from cortical cellular mechanisms. Early work suggested that neurons in lateral geniculate nucleus (LGN) are not affected by pattern adaptation (Derrington & Lennie, 1984; Maffei, Fiorentini, & Bisti, 1973), and these observations have been confirmed in cat visual cortex by Duong and Freeman (2007). However, Baccus and Meister (2002) showed clear contrast adaptation effects in the retina of the rabbit, and Solomon and colleagues (Solomon, Peirce, Dhruv, & Lennie, 2004) described contrast adaptation effects, specifically in M cells in the LGN, which can be traced to retinal ganglion cells. Their data suggest that, in primates at least, contrast adaptation occurs mainly in the retina for M cells and mainly in the cortex for P cells. It seems that adaptation is particularly strong at sites that pool responses from many neurons. Nevertheless, there remains some controversy as to whether signals from the retina may be normalised in some way for contrast (for a contemporary review of these issues see Webster, 2011). A number of studies have proved the existence of substantial adaptation in orientation-selective cortical neurons in cat striate cortex (Movshon & Lennie, 1979; Webster & De Valois, 1985) and macaque V1 (Sclar et al., 1989). More recently, Sapountzis, Schluppeck, Bowtell, and Peirce (2010) used two different fMRI techniques (adaptation and multivariate pattern classification analyses) to measure orientation selectivity in the human cortex. Selectivity to orientation was higher in early visual areas (V1, V2, and V3) than in higher areas. The orientation selectivity of the adaptation effects reported here are consistent with an early cortical locus. Since RTs to simple patterns are delineated by precortical mechanisms (Murray & Plainis, 2003; Plainis & Murray, 2000), our finding of spontaneous recovery suggests that the multiple controlling mechanisms of adaptation may exist as early as in V1.

#### 8.5 *Concluding remarks*

The central finding reported here is that, using simple RTs, it is possible to study the physiological mechanisms underlying pattern adaptation. From the results presented in this paper, it is clear that the RT data are broadly consistent with both psychophysical and the electrophysiological findings. Furthermore, the RT technique can provide insight into the time course of the recovery and allows the possibility to measure performance at a wide range of suprathreshold contrasts. In addition, the method allows evaluation of the effect of contrast adaptation by transforming RTs to effective contrast reduction, using RT-based contrast response functions. The above are of particular importance because they may provide additional information about the site of the many different forms of sensitivity adjustment that we call adaptation.

**Acknowledgments.** We thank subjects NK, VZ, and GB for participating in the experiments. NRAP's participation was facilitated by the Manchester Biomedical Research Centre and the Greater Manchester Comprehensive Local Research Network.

#### **References**

- Anderson, A. J., & McKendrick, A. M. (2007). Quantifying adaptation and fatigue effects in frequency doubling perimetry. *Investigative Ophthalmology & Visual Science*, **48**, 943–948.
- Baccus, S. A., & Meister, M. (2002). Fast and slow contrast adaptation in retinal circuitry. *Neuron*, **36**, 909–919.
- Bao, M., & Engel, S. A. (2012). Distinct mechanism for long-term contrast adaptation. *Proceedings of the National Academy of Sciences of the USA*, **109**, 5898–5903.

- 
- Bao, M., Fast, E., Mesik, J., & Engel, S. (2013). Distinct mechanisms control contrast adaptation over different timescales. *Journal of Vision*, **13**(10):14, 1–11.
- Blakemore, C., & Campbell, F. W. (1969a). Adaptation to spatial stimuli. *The Journal of Physiology*, **200**, 11P–13P.
- Blakemore, C., & Campbell, F. W. (1969b). On the existence of neurones in the human visual system selectively sensitive to the orientation and size of retinal images. *The Journal of Physiology*, **203**, 237–260.
- Blakemore, C., Muncey, J. P., & Ridley, R. M. (1973). Stimulus specificity in the human visual system. *Vision Research*, **13**, 1915–1931.
- Blakemore, C., & Nachmias, J. (1971). The orientation specificity of two visual after-effects. *The Journal of Physiology*, **213**, 157–174.
- Campbell, F. W., & Kulikowski, J. J. (1966). Orientational selectivity of the human visual system. *The Journal of Physiology*, **187**, 437–445.
- Daugman, J. G. (1985). Uncertainty relation for resolution in space, spatial frequency, and orientation optimized by two-dimensional visual cortical filters. *Journal of the Optical Society of America A*, **2**, 1160–1169.
- De Valois, K. K. (1977). Spatial frequency adaptation can enhance contrast sensitivity. *Vision Research*, **17**, 1057–1065.
- De Valois, R. L., & De Valois, K. K. (1990). *Spatial vision* (Oxford: Oxford University Press).
- Derrington, A. M., & Lennie, P. (1984). Spatial and temporal contrast sensitivities of neurones in lateral geniculate nucleus of macaque. *The Journal of Physiology*, **357**, 219–240.
- Duong, T., & Freeman, R. D. (2007). Spatial frequency-specific contrast adaptation originates in the primary visual cortex. *Journal of Neurophysiology*, **98**, 187–195.
- Georgeson, M. A., & Harris, M. G. (1984). Spatial selectivity of contrast adaptation: Models and data. *Vision Research*, **24**, 729–741.
- Gilinsky, A. S. (1968). Orientation-specific effects of patterns of adapting light on visual acuity. *Journal of the Optical Society of America*, **58**, 13–18.
- Greenlee, M. W., Georgeson, M. A., Magnussen, S., & Harris, J. P. (1991). The time course of adaptation to spatial contrast. *Vision Research*, **31**, 223–236.
- Greenlee, M. W., & Heitger, F. (1988). The functional role of contrast adaptation. *Vision Research*, **28**, 791–797.
- Greenlee, M. W., & Magnussen, S. (1988). Interactions among spatial frequency and orientation channels adapted concurrently. *Vision Research*, **28**, 1303–1310.
- Harwerth, R. S., & Levi, D. M. (1978). Reaction time as a measure of suprathreshold grating detection. *Vision Research*, **18**, 1579–1586.
- Hegde, J. (2009). How reliable is the pattern adaptation technique? A modeling study. *Journal of Neurophysiology*, **102**, 2245–2252.
- Heinrich, T. S., & Bach, M. (2002). Contrast adaptation in retinal and cortical evoked potentials: No adaptation to low spatial frequencies. *Visual Neuroscience*, **19**, 645–650.
- Klein, S. (1991). Channels: Bandwidth, channel independence, detection vs. discrimination. In B. Blum (Ed.), *Channels in the visual nervous system: Neurophysiology, psychophysics and models* (pp. 11–27). London: Freund.
- Kohn, A. (2007). Visual adaptation: Physiology, mechanisms, and functional benefits. *Journal of Neurophysiology*, **97**, 3155–3164.
- Ling, S., & Carrasco, M. (2006). When sustained attention impairs perception. *Nature Neuroscience*, **9**, 1243–1245.
- Maffei, L., Fiorentini, A., & Bisti, S. (1973). Neural correlate of perceptual adaptation to gratings. *Science*, **182**, 1036–1038.
- Mollon, J. D., & Polden, P. G. (1980). A curiosity of light adaptation. *Nature*, **286**, 59–62.
- Morgan, M. (2013). Sustained attention is not necessary for velocity adaptation. *Journal of Vision*, **13**(8):26, 1–11.
- Morgan, M. J. (2011). Wohlgenuth was right: Distracting attention from the adapting stimulus does not decrease the motion after-effect. *Vision Research*, **51**, 2169–2175.
- Movshon, J. A., & Lennie, P. (1979). Pattern-selective adaptation in visual cortical neurones. *Nature*, **278**, 850–852.

- Murray, I. J., & Plainis, S. (2003). Contrast coding and magno/parvo segregation revealed in reaction time studies. *Vision Research*, **43**, 2707–2719.
- Ohzawa, I., Sclar, G., & Freeman, R. D. (1982). Contrast gain control in the cat visual cortex. *Nature*, **298**, 266–268.
- Palmer, J., Huk, A. C., & Shadlen, M. N. (2005). The effect of stimulus strength on the speed and accuracy of a perceptual decision. *Journal of Vision*, **5**(5), 376–404.
- Parry, N. R., Murray, I. J., & McKeefry, D. J. (2008). Reaction time measures of adaptation to chromatic contrast. *Visual Neuroscience*, **25**, 405–410.
- Parry, N. R., Plainis, S., Murray, I. J., & McKeefry, D. J. (2004). Effect of foveal tritanopia on reaction times to chromatic stimuli. *Visual Neuroscience*, **21**, 237–242.
- Pianta, M. J., & Kalloniatis, M. (2000). Characterisation of dark adaptation in human cone pathways: An application of the equivalent background hypothesis. *The Journal of Physiology*, **528**, 591–608.
- Plainis, S., & Murray, I. J. (2000). Neurophysiological interpretation of human visual reaction times: Effect of contrast, spatial frequency and luminance. *Neuropsychologia*, **38**, 1555–1564.
- Plainis, S., & Murray, I. J. (2005). Magnocellular channel subserves the human contrast-sensitivity function. *Perception*, **34**, 933–940.
- Plainis, S., Parry, N. R. A., Sapountzis, P., Murray, I. J., & Pallikaris, I. G. (2006). The effect of contrast adaptation on visual reaction times (RTs): Spatial-frequency and orientation tuning. *Investigative Ophthalmology & Visual Science*, **47**, ARVO E-Abstract 5353.
- Ross, J., & Speed, H. D. (1991). Contrast adaptation and contrast masking in human vision. *Proceedings of the Royal Society of London B: Biological Sciences*, **246**, 61–69.
- Sapountzis, P., Schluppeck, D., Bowtell, R., & Peirce, J. W. (2010). A comparison of fMRI adaptation and multivariate pattern classification analysis in visual cortex. *NeuroImage*, **49**, 1632–1640.
- Sclar, G., Lennie, P., & DePriest, D. D. (1989). Contrast adaptation in striate cortex of macaque. *Vision Research*, **29**, 747–755.
- Sekuler, R. W. (1965). Spatial and temporal determinants of visual backward masking. *Journal of Experimental Psychology: General*, **70**, 401–406.
- Solomon, S. G., Peirce, J. W., Dhruv, N. T., & Lennie, P. (2004). Profound contrast adaptation early in the visual pathway. *Neuron*, **42**, 155–162.
- Stecher, S., Sigel, C., & Lange, R. V. (1973). Spatial frequency channels in human vision and the threshold for adaptation. *Vision Research*, **13**, 1691–1700.
- Stromeyer, C. F., 3rd, & Julesz, B. (1972). Spatial-frequency masking in vision: Critical bands and spread of masking. *Journal of the Optical Society of America*, **62**, 1221–1232.
- Stromeyer, C. F., 3rd, Klein, S., Dawson, B. M., & Spillmann, L. (1982). Low spatial-frequency channels in human vision: Adaptation and masking. *Vision Research*, **22**, 225–233.
- Taylor, M. J., Carpenter, R. H., & Anderson, A. J. (2006). A noisy transform predicts saccadic and manual reaction times to changes in contrast. *The Journal of Physiology*, **573**, 741–751.
- Tolhurst, D. J. (1972). Adaptation to square-wave gratings: Inhibition between spatial frequency channels in the human visual system. *The Journal of Physiology*, **226**, 231–248.
- Tolhurst, D. J., & Barfield, L. P. (1978). Interactions between spatial frequency channels. *Vision Research*, **18**, 951–958.
- Wark, B., Fairhall, A., & Rieke, F. (2009). Timescales of inference in visual adaptation. *Neuron*, **61**, 750–761.
- Webster, M. A. (2011). Adaptation and visual coding. *Journal of Vision*, **11**(5):3, 1–23.
- Webster, M. A., & De Valois, R. L. (1985). Relationship between spatial-frequency and orientation tuning of striate-cortex cells. *Journal of the Optical Society of America A*, **2**, 1124–1132.
- Wilson, H. R., & Humanski, R. (1993). Spatial frequency adaptation and contrast gain control. *Vision Research*, **33**, 1133–1149.
- Yeh, T., Lee, B. B., & Kremers, J. (1996). The time course of adaptation in macaque retinal ganglion cells. *Vision Research*, **36**, 913–931.